Estimates of Mixing

Jody M. Klymak Jonathan D. Nash

May 14, 2007

Abstract

Vertical fluxes of tracers and momentum in the ocean are dominated by turbulent transports. Since it is impossible to measure the complete set of motions associated with turbulent processes, estimates of mixing rely on sets of assumptions. In this article, we describe the most common techniques used for estimating ocean mixing, which may be based on (1) large- or (2) micro-scale observations.

Large-scale estimates may involve the purposeful release of a man-made tracer and the subsequent measurement of its release over time. Alternatively, transport budgets can be used to determine mixing if a closed system can be defined.

Microscale estimates generally rely on direct measurement of the turbulent motions and/or the consequences of these motions. Direct eddy correlations rely on quantifying the turbulent stirring. In contrast, the Osborn-Cox method quantifies the rate of irreversible molecular mixing associated with turbulent structures. The most commonly used microscale estimate (the Osborn method) assumes an energy balance in which turbulent energy production is balanced by turbulent buoyancy flux and viscous dissipation. Several variants on these techniques are also discussed, including mixing estimates from density overturns (Thorpe-scale analyses) and finescale shear based parameterizations (Gregg-Henyey/Polzin).

Introduction

Mixing in the ocean redistributes tracers, driving physical and biogeochemical dynamics. The mixing of the *active* tracers, temperature and salinity, changes the density of seawater, creating pressure gradients that drive mean currents. Circulations from small estuaries all the way up to the global overturning circulation are ultimately controlled by the mixing of buoyant fresh or warm water. Momentum is similarly diffused by turbulent mixing, which acts to transmit forces through the ocean surface and boundaries into the interior. The mixing of *passive* scalars like nutrients, carbon dioxide, and oxygen, is important to understanding biological cycles in the ocean. Phytoplankton rely on vertical mixing processes to transport recycled nutrients into the sunlit near-surface waters. The mixing of carbon dioxide ultimately affects its storage in the ocean and removal from the atmosphere.

In the interior of the ocean, most of the mixing takes place when internal waves break, driving dense water over light. Breaking is the result of instabilities of the internal wave flow due to focusing of wave energy. A numerical simulation of a shear instability (Smyth et al., 2001) illustrates the anatomy of a mixing event (figure 1). In this example, a Kelvin-Helmholtz billow is triggered from an initially

uniform shear-flow. As the flow evolves, a wave-like instability grows and rolls up into two vortices (a) that pair to create a single breaking event that is initially mostly two-dimensional (b). Further instabilities ensue, creating a fully turbulent and three-dimensional flow field (c).

Breaking events like this are important because molecular diffusivity on *large-scale* gradients (tens of meters) is very ineffective at mixing. Mixing is ultimately accomplished by molecular processes via Fickian diffusion, i.e., the irreversible flux of property C is proportional to its three-dimensional gradient and the molecular diffusion coefficient κ_C:

$$\mathbf{f}_C = -\kappa_C \nabla C. \tag{1}$$

For temperature, a thermodynamic tracer, $\kappa_T \approx 10^{-7}$ m^2 s^{-1} and for salinity and other tracers $\kappa_S \approx 10^{-9}$ m^2 s^{-1}. At large scales, representing the non-turbulent flow, gradients are small and the molecular flux is slow. However, the stirring driven by the breaking of *finescale* (order 10–1 m) waves, creates gradients at the *microscale* (order 1 cm–1 mm). The microscale gradients can be very large, as can be seen visually in figure 1b and c, and the molecular flux becomes significant.

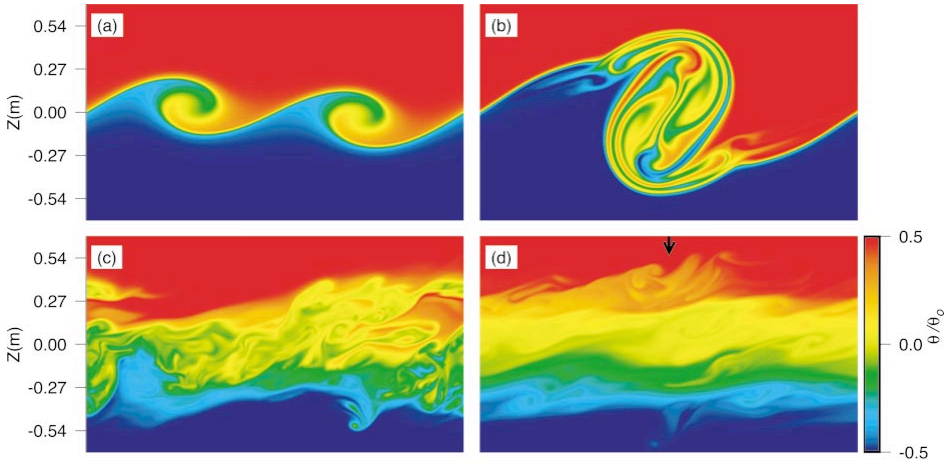

Figure 1: A numerical simulation of turbulent mixing (Smyth et al., 2001). The event is triggered by a shear instability between an upper layer of warm water (red) moving to the right and a layer of cold water (blue) moving to the left. The initial pair of vortices (a) pair to create a single large breaking event (b). This becomes fully turbulent and three dimensional (c) at which point there is large irreversible diffusion of the temperature. Diffusion continues until a large volume of mixed fluid results (d).

In this example, and in the ocean in general, turbulence acts to stir the fluid, greatly increasing the flux due to mixing, $\mathbf{F}_C$. It is very useful to parametrize the turbulent flux in terms of gradients of the mean fields $\overline{C}$. We do this by defining a *turbulent diffusivity* K_C so that

$$\mathbf{F}_C \approx -K_C \nabla \overline{C}. \tag{2}$$

Note that this parametrization has the same form as equation (1), so we are drawing a direct analogy between the random walk that accomplishes mixing on microscales and the stirring that takes place on the finescale of a breaking wave. The power of this concept is that the random walk of the stirring is on "large" scales, and does not change for different tracers in the water. Our model of turbulence assumes that all variance created via stirring at large scales is ultimately transformed to small enough scales where it diffuses via molecular processes. Thus, an estimate of the turbulent diffusivity for one tracer may be applied to other tracers experiencing the same turbulent flow, so that the turbulent diffusivity K is a dynamic property of the flow.

Approaches to Quantifying Mixing

The Advection-Diffusion Balance The sequence of events shown in figure 1 nicely illustrates different methods of how we quantify mixing in the ocean. Suppose we are interested in the mixing of temperature T in a fluid. It is often assumed that one can separate the scales of turbulent motions from those of the mean flow, allowing one to write:

$$T = \overline{T} + T' \tag{3}$$

$$\mathbf{u} = \overline{\mathbf{u}} + \mathbf{u}', \tag{4}$$

where the primes represent the "turbulent" part of the flow and the overbars the mean quantities. In figure 1, the horizontally averaged velocity and temperature represent the mean, and deviations from these the turbulence. This so-called "Reynolds decomposition" allows us to transform the advection-diffusion equation $\partial T/\partial t + \mathbf{u}\cdot\nabla T = \kappa_T \nabla^2 T$ into an evolution equation for the mean temperature $\overline{T}$:

$$\frac{\mathrm{D}\overline{T}}{\mathrm{Dt}} = \kappa_T \nabla^2 \overline{T} + \nabla \cdot \left\langle \mathbf{u}' T' \right\rangle \tag{5}$$

$$= -\nabla \cdot (\mathbf{f}_T + \mathbf{F}_T). \tag{6}$$

Here, the material derivative $\mathrm{D}/\mathrm{Dt} = (\partial/\partial t + \overline{\mathbf{u}}\cdot\nabla)$ is the change in time following a parcel in the mean flow, and the angle brackets are an average in time and space over a turbulent event. Equation (5) shows that $\overline{T}$ depends not only on $\overline{T}$ and $\overline{u}$, but also on the correlation $\langle \mathbf{u}' T' \rangle$ which we term the turbulent heat flux, often approximated using the Fickian analogy (2) as:

$$\mathbf{F}_T = -\left\langle \mathbf{u}' T' \right\rangle \approx -K \nabla \overline{T}. \tag{7}$$

In most places in the ocean, the turbulent flux acting on the mean gradients is much greater than the molecular one, $|\mathbf{F}_T| >> |\mathbf{f}_T|$, implying that we can drop the first term on the right-hand side of equation (5).

Considering figure 1 again, suppose we integrate over a volume defined by the lower half of the domain, with z=0 the top of the volume. There are no fluxes out the sides or bottom of the volume, and there is no mean flux out the top ($w(z = 0) = 0$). The only flux of temperature is the turbulent one through z=0, so that the change of temperature in the volume can be calculated by:

$$\frac{\partial}{\partial t} \int_V \overline{T} \, \mathrm{d}V = -\oint_A \left\langle w' T' \right\rangle \mathrm{d}A, \tag{8}$$

where A is the surface at z=0. In figure 1, there is an increase in the mean temperature of the volume, so the left-hand side of equation (8) is greater than zero. The tendrils that drop below z=0 are warmer than the mean, so $T' > 0$, and they are moving down, so $w' < 0$, therefore $w'T' < 0$. If the tendrils are completely diffused away by molecular mixing, then warm water will have been left behind in our volume and the temperature will have increased due to mixing. The real situation is more complicated. Tendrils are further strained and stretched, and some of the warm water rises again out of the volume. However, on average some is always exchanged so that $\langle w'T' \rangle < 0$ and net warming takes place in the lower volume. Note that there is an equal amount of cooling in the upper volume.

The Gradient-Variance Balance In order for stirring to be irreversible, the gradients produced must be diffused away by molecular processes. For temperature, this is described formally through the evolution equation for turbulent temperature-gradient variance $|\nabla T'|^2$. Temperature-gradient variance is a non-intuitive quantity to consider, but it is the best measure of "stirring", and is intimately related with the thermodynamic quantity of entropy (Eckart, 1948). For steady-state, homogeneous turbulence it can be shown that:

$$-\left\langle \mathbf{u}'T' \right\rangle \cdot \nabla \overline{T} \approx \kappa_T \left\langle \left| \nabla T' \right|^2 \right\rangle. \tag{9}$$

This states that the net production of gradient variance by turbulent velocities is balanced by its destruction by molecular diffusion (there are transport terms that have been dropped, hence the approximation). Again, the averages represented by the angle brackets must be collected over long enough time that the irreversible part of the "turbulent" flux is measured. The rate of destruction of the turbulent gradients is fundamental to quantifying mixing in the ocean and is written as:

$$\chi_T \equiv 2\kappa_T \left\langle \left| \nabla T' \right|^2 \right\rangle. \tag{10}$$

Large-scale estimates

Large-scale estimates are made on quantities measured on vertical scales greater than a meter. They are based on estimating the mixing terms in the advection-diffusion equation of the tracer $\overline{C}$

$$\frac{\partial \overline{C}}{\partial t} + \mathbf{u} \cdot \nabla \overline{C} = \nabla \cdot (K \nabla \overline{C}), \tag{11}$$

where again, K is the turbulent diffusivity. Often the right-hand side is replaced by $\partial/\partial z(K \partial \overline{C}/\partial z)$ because mean vertical gradients exceed horizontal ones, further reducing to $K\partial^2 \overline{C}/\partial z^2$ for constant K.

Purposeful Tracer Releases

The first and conceptually simplest method to measure mixing is to release a man-made tracer and measure its vertical spread over time. If we follow the parcel of

water and assume a constant vertical diffusivity K, then the spread of the tracer, $\overline{C}$, is governed by the diffusion equation

$$\frac{\partial \overline{C}}{\partial t} = K \frac{\partial^2 \overline{C}}{\partial z^2}. \tag{12}$$

If the tracer is injected as a delta function at $t = 0$, then the solution is an ever-widening vertical cloud described by a Gaussian. The larger K, the faster the cloud spreads.

It is only necessary to track the vertical spread of the dye to estimate the turbulent diffusivity K. The stratification of the ocean suppresses mean vertical flow, so turbulence is the only effective mechanism that causes vertical spreading of the patch. The dye will also spread horizontally, however most of this is due to reversible non-turbulent motions such as eddies and mesoscale straining. These horizontal motions constitute an important stirring mechanism on large scales, but do not accomplish strong irreversible mixing until turbulence acts on them. [1]

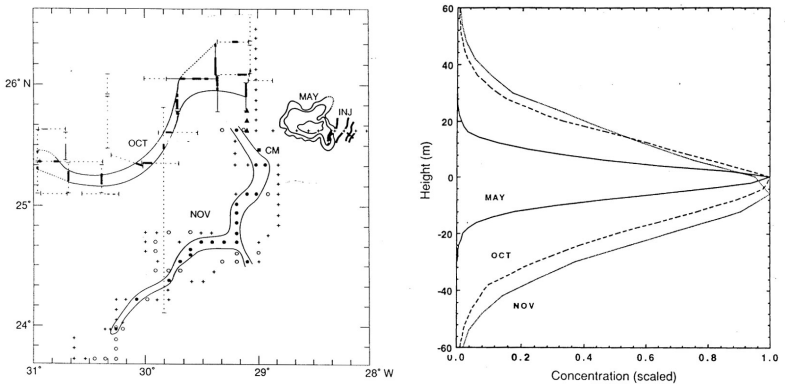

Figure 2: Vertical spread of a man-made tracer SF_6 in the open-ocean thermocline (Ledwell et al., 1993) a) Shows the lateral location and spread of the dye at the time of injection, six, and seven months later. The dye patch has been strained by mesoscale processes from its initial small injection region in May. b) shows the vertical spread of the dye averaged over the lateral spread. The widening of the Gaussian between May and November is consistent with a diapycnal diffusivity of $K = 0.11 \times 10^{-4}\,\mathrm{m^2\,s^{-1}}$.

Tracer is released on a surface of constant density, and then returned to later and to be remeasured and compared to the original distribution (Ledwell et al., 1993). The example shown here is from the open ocean thermocline where sulfur-hexafluoride (SF_6) was injected on a density surface at 310 m depth (figure 2). Horizontal motions strained the dye patch into thin horizontal tendrils, as seen during three repeat surveys several months later (figure 2a). However, when averaged horizontally, the vertical distribution of the dye conformed very well to the Gaussian spread predicted from the solution of equation (5). From the rate of

[1] Care should be taken interpreting the terms "vertical" and "horizontal" or "lateral". By these terms, we really mean perpendicular and parallel to surfaces of constant density respectively, or *isopycnal* and *diapycnal*. Doing this is conceptually important, but notationally less convenient, so we do not do so here.

spread, Ledwell et al. (1993) found a turbulent diffusivity of $K = 10^{-5}$ m^{2}s^{-1}, at least one order of magnitude greater than molecular. A similar experiment in the semi-enclosed Brazil Basin found an average turbulent diffusivity of $K = 0.5 \times 10^{-4}$m^{2}s^{-1} (Polzin et al., 1997).

Direct tracer releases are elegant and definitive in their results. There are no confounding sources or sinks of the dye in the ocean, so tracking the vertical spread is unambiguous. But the technique is difficult to perform. Specialized equipment and analysis methods are needed to release the dye and then analyze the water samples to find minute quantities of tracer in the water. Horizontal stirring and advection of a dye patch can spread it horizontally to such an extent that it is very difficult to find all the dye using finite ship resources, as should be clear from the 100-km scales of figure 2a.

Tracer Budgets (Inverse Methods)

The rate of mixing can be estimated from an integrated version of the mean tracer equation (equation (11)) if we constrain a volume of water and assume its contents are in steady state. A concrete example of the budget method is from data collected in the Brazil Basin in the Southwest Atlantic (Hogg et al., 1982). Here, water colder than 1 °C produced in the Antarctic flows north into the basin through the Vema Channel (figure 3). No water that cold leaves the basin. Thus, the cold water must be warmed before it leaves the basin.

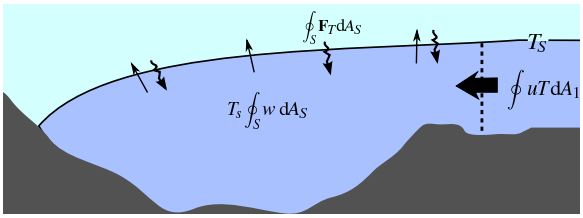

Figure 3: Sketch of heat fluxes in and out of a volume bounded in the vertical by an isotherm T_s, and at a strait by the dashed line.

Quantitatively, the mixing estimate is made by integrating the remaining terms in equation (11) over the volume:

$$\overbrace{\oint_1 \overline{u}\overline{T}\,\mathrm{d}A_1}^{in\ Vema} - \overbrace{\oint_S \overline{w}\overline{T_s}\,\mathrm{d}A_S}^{Adv.\ top} = \overbrace{\oint_S \mathbf{F}_T\,\mathrm{d}A_s}^{Turb.\ top}. \tag{13}$$

We also know that there is just as much water entering the volume as leaving through the upper surface, so $Q_S = Q_1$, where

$$Q_S = \oint_S \overline{w}\,\mathrm{d}A_S, \tag{14}$$

and Q_1 is similarly defined. Only the advective transport of heat into the basin needs to be measured (the l.h.s. of (13)) to determine the turbulent heat flux

through the upper bounding surface. Using a combination of moorings and shipboard cruises, Hogg et al. (1982) estimated these transports by assuming the deviations from the mean temperature and velocity values entering Vema Channel are uncorrelated:

$$\oint_1 \overline{u}\overline{T}\, \mathrm{d}A_1 \approx Q\left\langle \overline{T_1} \right\rangle .$$

They then defined the upper surface as the $T_S = 1\ ^\circ\mathrm{C}$ isotherm and assumed a constant vertical temperature gradient along that surface, allowing the mean turbulent diffusivity at that surface to be determined as

$$\overline{K} = \frac{Q}{A_s}(\overline{T_s} - \left\langle \overline{T_1} \right\rangle) \left\langle -\partial \overline{T}/\partial z \right\rangle^{-1} . \tag{15}$$

For the Brazil Basin, $Q = 3.7 \times 10^6\ \mathrm{m}^3 s^{-1}$, $A_S = 5 \times 10^{12}\ \mathrm{m}^2$, $\left\langle \overline{T_1} \right\rangle = 0.35^\circ\mathrm{C}$, and the mean temperature gradient at the $1\,^\circ\mathrm{C}$ surface is $-2 \times 10^{-3\circ}\mathrm{C\,m}^{-1}$, then the mean turbulent diffusivity across this interface is $\overline{K} \approx 2.5 \times 10^{-4}\,\mathrm{m^2 s^{-1}}$ (Hogg et al., 1982).

Inverse estimates of mixing are routinely made from hydrographic sections in the ocean, where the same concepts are used to find the flux of heat and density at different depths in a series of volumes (i.e. Ganachaud and Wunsch, 2000; Lumpkin and Speer, 2003). Often many vertical layers and sections are used. If well-constrained, this method of estimating the heat flux (and thus the diapycnal mixing) would be unambiguous in providing basin-average estimates. For example, Munk (1966) used a one-dimensional advection-diffusion balance to estimate the turbulent diffusivity in the deep ocean from large-scale tracer profiles. Recently updated by Munk and Wunsch (1998), these inverse estimates of the North Pacific find average turbulent diffusivities of $K = 10^{-4}\ \mathrm{m^2\,s^{-1}}$.

The principal difficulty with the inverse method is the assumption that the system is in steady state. Inverse estimates in the open ocean indicate vertical velocities of a couple of meters-per-year. This is a difficult amount of change to detect in open-ocean basins with any confidence. Furthermore, the velocities and tracers measured at the boundaries of the volume must be well-constrained and shown to be in steady state. This is very difficult as velocities and tracers are estimated from a scarce individual ship tracks that each take a month or more to complete, often months or years apart. Not surprisingly, the most convincing inverse estimates have come from well-constrained topographies like the Brazil Basin where the flow and temperatures into the basin can be monitored with a few long-term moorings in the channel, and the bounding isotherm can be mapped with a high degree of confidence.

Fine- and microscale estimates

Fine- and microscale measurements estimate turbulent stirring or mixing by directly observing the turbulence. These methods have the advantage over budget-based estimates in that they elucidate what causes the turbulence. However, these methods require specialized instrumentation as the sensors used to measure microscale quantities must be small, respond quickly, and be capable of recording a very large dynamic range. In addition, the vehicles they are mounted on must suppress vibrations as much as possible to prevent contaminating the small-scale signals (figure 4).

In the following, we describe a series of methods that (1) directly measure the turbulent stirring of a fluid using the eddy correlation technique, (2) directly measure the molecular destruction of temperature gradients, (3) estimate the mixing by relating the buoyancy-flux to the energetics of the turbulence. Finally, we describe two techniques that enable mixing to be estimated from large-scale measurements of (1) statically unstable fluid (Thorpe-scales), and (2) energy in the internal wavefield (the Gregg-Henyey method).

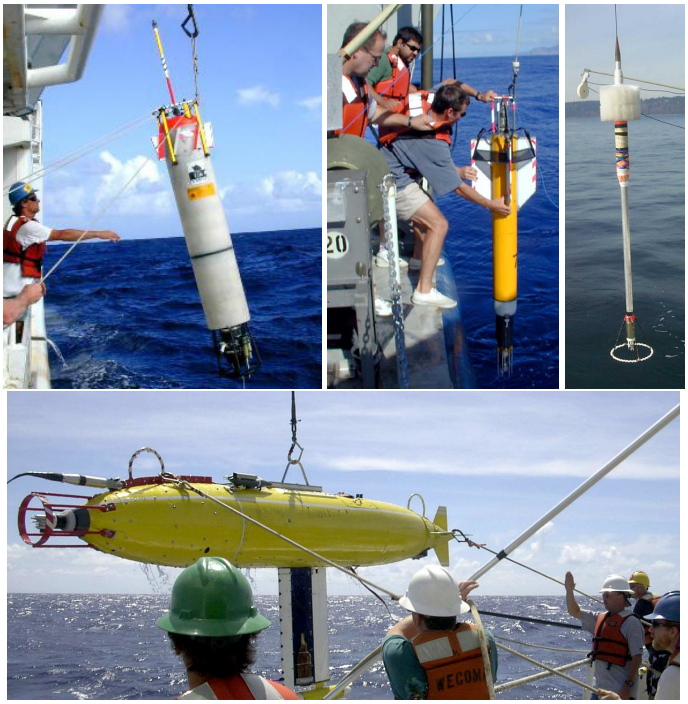

Figure 4: A menagerie of microstructure platforms that the authors have worked with. In all cases the sensors are on the nose of the vehicles. The upper three are profilers, the lower instrument is towed.

Direct Eddy Correlation

With careful and specialized measurements it is possible to estimate mixing by quantifying the stirring of the fluid. As described above, this means quantifying the stirring of cold water upward into warm water by measuring vertical velocity fluctuations, w' and temperature fluctuations T'.

One of the few attempts to apply this method in the open ocean (Fleury and Lueck, 1994) demonstrates its difficulty (figure 5). Temperature and velocity were acquired along a horizontal path using a towed instrument outfitted with thermistors and shear probes. While the raw signals are large and very active (figure 5a), the product $w'T'$ is not one-sided. Instead, it has instantaneous values that are large and can be of either positive and negative sign, such that the fluctuations are

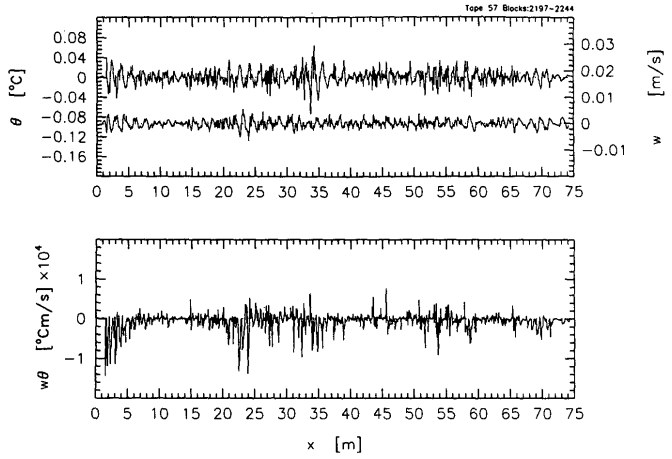

Figure 5: Upper panel: Spatial series of high-passed temperature and vertical velocity from a towed vehicle in the upper ocean thermocline (Fleury and Lueck, 1994). The high-passing procedure is meant to emphasize turbulent fluctuations. Lower panel: The correlation between these observations.

far greater than the mean correlation $\langle w'T' \rangle$. This is a general problem since turbulence is sporadic, and stirring is both down-gradient (i.e., transports heat from regions of warm fluid) and up-gradient (i.e., transports heat *to* regions of warm fluid), the latter presumably representing restratification of partially mixed fluid. Since much of $w'T'$ is reversible (i.e., just stirring fluid that is not immediately mixed), the eddy-correlation technique must be made over long times to produce stable estimates of the irreversible flux. In this case, the background vertical gradient $d\overline{T}/dz$ is positive, so $\langle w'T' \rangle < 0$ represents a down-gradient flux, as appears most frequently in figure 5b.

This method does not enjoy wide use. Determining what is "mean" and what is "turbulent" is very difficult from the limited measurements possible with a vertical or horizontal profiler. The data presented here was simply bandpassed, with large scale motions considered to be non-turbulent. However choosing what is "large scale" requires some art. A second difficulty is estimating the vertical velocities in the ocean. In this instance, the vertical velocities were $w' \approx 0.03$ m s^{-1}, large enough that the method was deemed possible. The final limitation is gathering enough statistics of the turbulence to make estimates of mean fluxes.

Microscalars (Osborn-Cox method)

In contrast to measuring the finescale stirring of the tracer (i.e., $\langle w'T' \rangle$ above), the Osborn-Cox method quantifies the rate of molecular diffusion of scalar variance at the microscale. By considering the evolution equation for microscale scalar variance, Osborn and Cox (1972) showed that turbulent diffusivity K is related to the rate of destruction of scalar variance χ (equation (10)). Because this method measures the rate of irreversible molecular mixing, it is one of the most direct

measures of quantifying K.

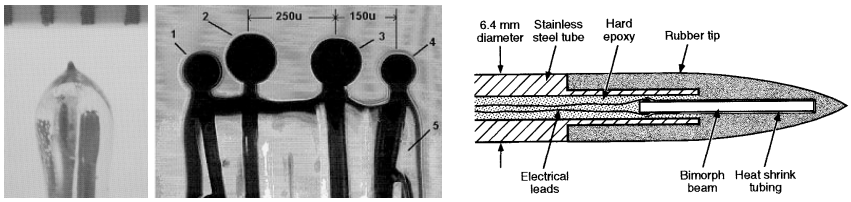

Figure 6: Three common sensors used on microstructure instruments. Left: A glass bead thermistor. The upper scale is in millimeters (Gregg, 1999). Center: a four-electrode microconductivity probe (Nash and Moum, 1999). Right: Schematic of a piezo-electric shear probe (Gregg, 1999).

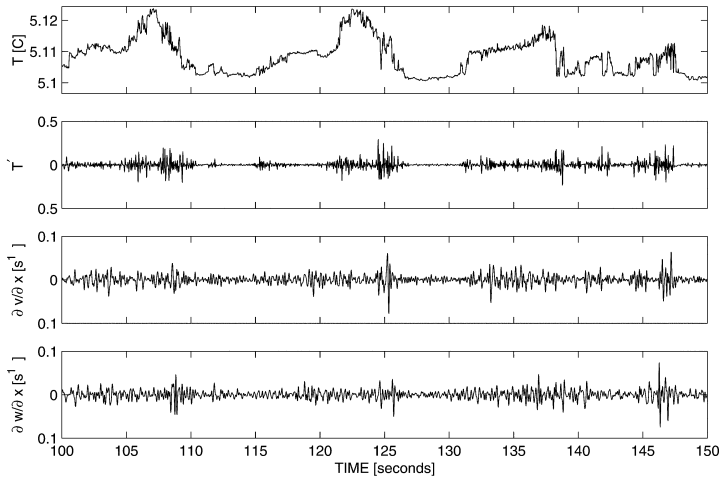

Figure 7: Data collected using a towed vehicle in the open ocean (Moum et al., 2002). This data was collected with the instrument moving at $1\,\mathrm{m\,s^{-1}}$, so time and spatial derivatives are approximately the same. a) Temperature b) temperature gradient, c) and d) velocity gradients (shear). Note that where there is high velocity variance there is usually high temperature variance.

The most commonly measured scalar is temperature, as it is relatively easy to measure and diffuses at larger scales (i.e., 1mm-1cm) than chemical constituents like salt. To measure such scales, a sensor must be small and respond very rapidly. Microbead thermistors – coated with a thin film of glass to electrically insulate them from seawater (figure 6) – are generally used for this purpose. This sensor yields high-resolution temperature gradients such as those shown in (figure 7b). Only one dimension of the gradient is measured, so we estimate χ as:

$$\chi = 6\kappa_T \left\langle \left(\frac{\partial T'}{\partial z} \right)^2 \right\rangle, \tag{16}$$

where we have assumed that the turbulence is isotropic ($\partial T'/\partial x = \partial T'/\partial y = \partial T'/\partial z$). The turbulent diffusivity simply relates the intensity of small-scale gradients to the large-scale temperature gradient as

$$K = 3\kappa_T \frac{\langle (\partial T'/\partial z)^2 \rangle}{\left(\partial \overline{T}/\partial z\right)^2} = \frac{\chi}{2\left(\partial \overline{T}/\partial z\right)^2}. \tag{17}$$

Like other methods, there are a number of limitations. Temperature probes require a finite amount of time to diffuse heat through their insulation and the thermal boundary that develops in the surrounding seawater. This smooths the signals and coarsens the measurement of small-scale gradients. If probes can be lowered slowly enough to allow heat to diffuse through the coating, but fast enough to capture a synoptic snapshot of the turbulent event, then all of the gradient variance could be resolved and χ measured. However, the required 10-20 cm/s profiling speed reduces the number of realizations that may be captured, so there is a tradeoff between resolution and statistics. In practice, most sensors are deployed too rapidly and not all of the variance is measured. Corrections can be applied by fitting data to a universal spectrum (i.e., the *Batchelor* or *Kraichnan* spectrum) which allows extrapolation of resolved measurements to higher wavenumbers (figure 8). Unfortunately, the spectral levels and wavenumber extent of the spectrum both depend on the turbulent kinetic energy dissipation rate ε, so an independent measure of microscale shear variance is required to accurately apply such corrections (Gregg, 1999).

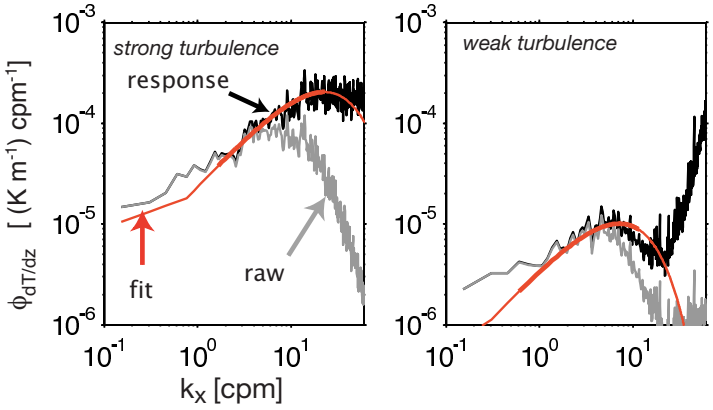

Figure 8: Fit of universal turbulence spectra (red curves) to data spectra collected near Hawaii (Klymak and Moum, 2007). The raw signals (gray) have been corrected (black) for the temporal response of the thermistor.

It is also possible to use microconductivity probes to measure temperature on spatial scales of 10^{-3} m (figure 6b). Conductivity is a rapid measurement, so speed through the water does not limit probe response, only the physical configuration of the probes. The difficulty with this measurement is that conductivity depends on both the temperature and salinity of seawater. Thus, microconductivity works

best for determining the mixing rate of temperature in water that has small salinity variations (Nash and Moum, 1999).

The last difficulty, shared with the other microscale methods is that turbulence is intermittent, so a large number of samples needs to be made in order to characterize the turbulence level of a given locale. However, unlike the estimate $\langle w'T' \rangle$, χ is a direct measure of irreversible mixing, so does not need many realizations of the same turbulent event.

Estimates from energy considerations (Osborn method)

The most common method of estimating ocean mixing rates is based on quantifying the energetics of the turbulence, not the mixing itself. It is widely employed because measurements can be obtained from rapidly profiling sensors, and because energy measurements are useful in their own right. This method was originally proposed by Osborn (1980), and is based on the observation that temperature-gradient variance occurs in accord with velocity gradient (shear) variance (i.e., compare figure 7b and c).

The argument is energetic. A turbulent event loses energy by viscous dissipation and by changing the background potential energy of the flow due to irreversible mixing. In a steady state, or time-averaged sense, this is expressed as

$$P = \varepsilon + J_b \tag{18}$$

where P is the rate of production of turbulence by the mean flow due to some wave-breaking process, ε is the rate of energy dissipation, and J_b is the irreversible buoyancy flux due to mixing. The buoyancy flux is directly related to the turbulent mass flux $J_b = g \langle \rho' w' \rangle / \overline{\rho}$ where g is the gravitational acceleration, and $\rho = \overline{\rho} + \rho'$ is the density.

The method assumes that the turbulent buoyancy flux is a fixed ratio of the dissipation:

$$J_b \approx \Gamma \varepsilon. \tag{19}$$

This is a somewhat bold assumption as obvious counter-examples can be found. For instance, in unstratified water, the buoyancy flux must be zero by definition, but ε can be substantial. However, observations indicate that for much of the stratified ocean the "mixing efficiency" $\Gamma \approx 0.2 \pm 0.05$.

Measurements of the dissipation rate of turbulent kinetic energy ε are made from microstructure profilers (figure 4) in much the same way that measurements of χ are made. A small shear probe (figure 6c) measures velocity shear (figure 7c and d). The shear variance is integrated to get an estimate of the dissipation rate of turbulent kinetic energy ε, again sometimes using universal spectra as a guide (Moum et al., 1995; Gregg, 1999). Fortunately, both the spectral amplitude and wavenumber extent of shear spectra scale with ε, so that universal spectra may be fit to a limited range of wavenumber range of the shear spectrum. But unlike the measurement of χ using thermistors, measurement of turbulent shear variance is easily contaminated by the slightest vibration of the measurement platform. This necessitates the use of specialized profilers that minimize coherent eddy shedding and decouple ship motion from the sensor (figure 4).

Just like temperature, the flux of density can be parametrized by a turbulent diffusivity so that:

$$J_b = -\frac{g}{\rho_0} K \frac{\partial \overline{\rho}}{\partial z} = K N^2, \tag{20}$$

for stratification $N^2 = -\frac{g}{\rho_o}\frac{d\rho}{dz}$. Combining, we use measurements of ε to estimate:

$$K = \Gamma \frac{\varepsilon}{N^2}. \tag{21}$$

This method has greatly increased the number of estimates of mixing in the ocean. Microstructure profilers have been deployed in a wide array of environments, from the open ocean, over rough and abrupt topography, and in coastal waters, giving us a large varieties of environments in which ocean mixing has been estimated. As tenuous as it is, the assumptions used in this method are mitigated by the fact that we know that dissipation rates vary by orders of magnitude worldwide and maps of dissipation are roughly a map of mixing.

Thorpe Scales The dissipation rate can be estimated from less specialized instruments. Breaking internal waves, like that shown in figure 1, lift dense water above light water. The dissipation rate of the water that goes into turbulence from this uplift can be estimated from the size of the overturn L_T:

$$\varepsilon \approx 0.8 L_T^2 N^3. \tag{22}$$

This has been shown to give unbiased estimates of the dissipation rate if enough profiles are collected (Dillon, 1982; Moum, 1996). Note that, at open-ocean dissipation rates and stratifications, L_T is quite small and the small density differences make detecting overturns subject to noise constraints (see Johnson and Garrett, 2004, for a recent discussion).

A coastal example is shown in figure 9, where braids indicative of shear-instabilities drive density overturns with $L_T \approx 5$ m. The overturns coincide with strong turbulence (Seim and Gregg, 1994). There is also a strong correspondence of ε and χ in these data. This study compared the two estimates of K from these separate microstructure estimates and found similar results.

Gregg-Henyey method The Osborn method is extended further using the observation that the dissipation rate is directly related to the energy in the internal wave field, the presumed source of most open-ocean turbulence (Gregg, 1989). Models have been developed that estimate the rate at which energy cascades through a steady-state internal wavefield (Henyey et al., 1986). It is easier to estimate the energy of the wavefield with finescale sensors than it is to directly measure the microscale. For instance, these methods have allowed the estimate of mixing using routine hydrographic data of the worlds oceans (Kunze et al., 2006, which also contains a recent review of the method). The internal-wave energy method has limited application in regions where the internal wavefield is not in equilibrium with external forcing, in particular near topography (Klymak et al., 2007), or where turbulence is generated by non-internal wave process at boundaries. Somewhat frustratingly, this is where the dissipation rates are the strongest.

Summary

Substantial effort has gone into estimating the rate of mixing in the ocean. The problem is very hard to tackle directly, so great ingenuity has been used to devise indirect methods of solving the problem observationally. Mixing measurements

have been made in many environments in the open and coastal ocean, lakes, and estuaries. In the Brazil Basin, where the source of deep water is well-constrained, estimates of K from the basin-scale estimates agree quite well with microstructure estimates (see for a nice summary St. Laurent et al., 2001). In the open ocean, however, large-scale and microscale methods do not agree as well. Inverse methods indicate turbulent diffusivities on the order of $K = 10^{-4}$ m^2 s^{-1}, while microstructure measurements are challenged to find turbulent diffusivities this high in the open ocean (see Wunsch and Ferrari, 2004, for a review). Recent attention has been directed towards finding enhanced mixing near boundaries (Klymak et al., 2006; Nash et al., 2007). This zeroth-order problem will continue to require much effort and ingenuity to solve. Higher order testing of the assumptions that go into these measurements are ongoing, aided by innovations in measurements and numerical methods.

Glossary of Terms

ε - rate of turbulent kinetic energy dissipation
K - turbulent diffusivity
N - buoyancy frequency
χ - rate of temperature variance dissipation
J_b - turbulent buoyancy flux
Γ - turbulent mixing efficiency
κ_C - molecular diffusivity for scalar C
$\mathbf{f_C}$ - turbulent flux of scalar C.

References

Dillon, T. M., 1982: Vertical overturns: A comparison of Thorpe and Ozmidov length scales. *J. Geophys. Res.*, **87**, 9601–9613.

Eckart, C., 1948: An analysis of the stirring and mixing processes in incompressible fluids. *J. Mar. Res.*, **7**, 265–275.

Fleury, M., and R. Lueck, 1994: Direct heat flux estimates using a towed vehicle. *J. Phys. Oceanogr.*, **24**, 810–818.

Ganachaud, A., and C. Wunsch, 2000: Improved estimates of global ocean circulation, heat transport and mixing from hydrographic data. *Nature*, **408**, 453–457.

Gregg, M. C., 1989: Scaling turbulent dissipation in the thermocline. *J. Geophys. Res.*, **94**, 9686–9698.

— 1999: Uncertainties in measuring ε and χ_t. *J. Atmos. Ocean. Tech.*, **16**, 1483–1490.

Henyey, F. S., J. Wright, and S. M. Flatté, 1986: Energy and action flow through the internal wave field. *J. Geophys. Res.*, **91**, 8487–8495.

Hogg, N., P. Biscaye, W. Gardner, and W. J. Schmitz, Jr., 1982: On the transport and modification of Antarctic bottom water in the Vema Channel. *J. Mar. Res.*, **40**, 231–263.

Johnson, H. L., and C. Garrett, 2004: Efffects of noise on Thorpe scales and run lengths. *J. Phys. Oceanogr.*, **34**, 2359–2373.

Klymak, J. M., and J. N. Moum, 2007: Interpreting spectra of horizontal temperature gradients in the ocean: Part II - turbulence. *J. Phys. Oceanogr.*, **37**, 1232–1245.

Klymak, J. M., J. N. Moum, J. D. Nash, E. Kunze, J. B. Girton, G. S. Carter, C. M. Lee, T. B. Sanford, and M. C. Gregg, 2006: An estimate of tidal energy lost to turbulence at the Hawaiian Ridge. *J. Phys. Oceanogr.*, **36**, 1148–1164.

Klymak, J. M., R. Pinkel, and L. N. Rainville, 2007: Direct breaking of the internal tide near topography: Kaena Ridge, Hawaii, in press, *J. Phys. Oceanogr.*

Kunze, E., E. Firing, J. M. Hummon, T. K. Chereskin, and A. M. Thurnherr, 2006: Global abyssal mixing inferred from lowered ADCP shear and CTD strain profiles. *J. Phys. Oceanogr.*, **36**, 1553–1576.

Ledwell, J., A. Watson, and C. Law, 1993: Evidence for slow mixing across the pycnocline from an open-ocean tracer-release experiment. *Nature*, **364**, 701–703.

Lumpkin, R., and K. Speer, 2003: Large-scale vertical and horizontal circulation in the North Atlantic Ocean. *J. Phys. Oceanogr.*, **33**, 1902–1920.

Moum, J. N., 1996: Energy-containing scales of turbulence in the ocean thermocline. *J. Geophys. Res.*, **101**, 14095–14109.

Moum, J. N., D. R. Caldwell, J. D. Nash, and G. D. Gunderson, 2002: Observations of boundary mixing over the continental slope. *J. Phys. Oceanogr.*, **32**, 2113–2130.

Moum, J. N., M. C. Gregg, R. C. Lien, and M. Carr, 1995: Comparison of turbulence kinetic energy dissipation rate estimates from two ocean microstructure profilers. *J. Atmos. Ocean. Tech.*, **12**, 346–366.

Munk, W., and C. Wunsch, 1998: Abyssal recipes II: energetics of tidal and wind mixing. *Deep Sea Res.*, **45**, 1977–2010.

Munk, W. H., 1966: Abyssal recipes. *Deep Sea Res.*, **13**, 707–730.

Nash, J., M. Alford, E. Kunze, K. Martini, and S. Kelley, 2007: Hotspots of deep ocean mixing on the oregon continental slope. *Geophys. Res. Lett.*, **34**, L01605, doi:10.1029/2006GL028170.

Nash, J. D., and J. N. Moum, 1999: Estimating salinity variance dissipation rate from conductivity measurements. *J. Atmos. Ocean. Tech.*, **16**, 263–274.

Osborn, T. R., 1980: Estimates of the local rate of vertical diffusion from dissipation measurements. *J. Phys. Oceanogr.*, **10**, 83–89.

Osborn, T. R., and C. S. Cox, 1972: Oceanic fine structure. *Geophys. Fluid Dyn.*, **3**, 321–345.

Polzin, K., J. Toole, J. Ledwell, and R. Schmitt, 1997: Spatial variability of turbulent mixing in the abyssal ocean. *Science*, **276**, 93–96.

Seim, H. E., and M. C. Gregg, 1994: Detailed observations of a naturally occurring shear instability. *J. Geophys. Res.*, **99**, 10049–10073.

Smyth, W. D., J. N. Moum, and D. R. Caldwell, 2001: The efficiency of mixing in turbulent patches: Inferences from direct simulations and microstructure observations. *J. Phys. Oceanogr.*, **31**, 1969–1992.

St. Laurent, L. C., J. M. Toole, and R. W. Schmitt, 2001: Buoyancy forcing by turbulence above rough topography in the abyssal Brazil Basin. *J. Phys. Oceanogr.*, **31**, 3476–3495.

Wunsch, C., and R. Ferrari, 2004: Vertical mixing, energy, and the general circulation of the oceans. *Ann. Rev. Fluid Mech.*, **36**, 281–314.

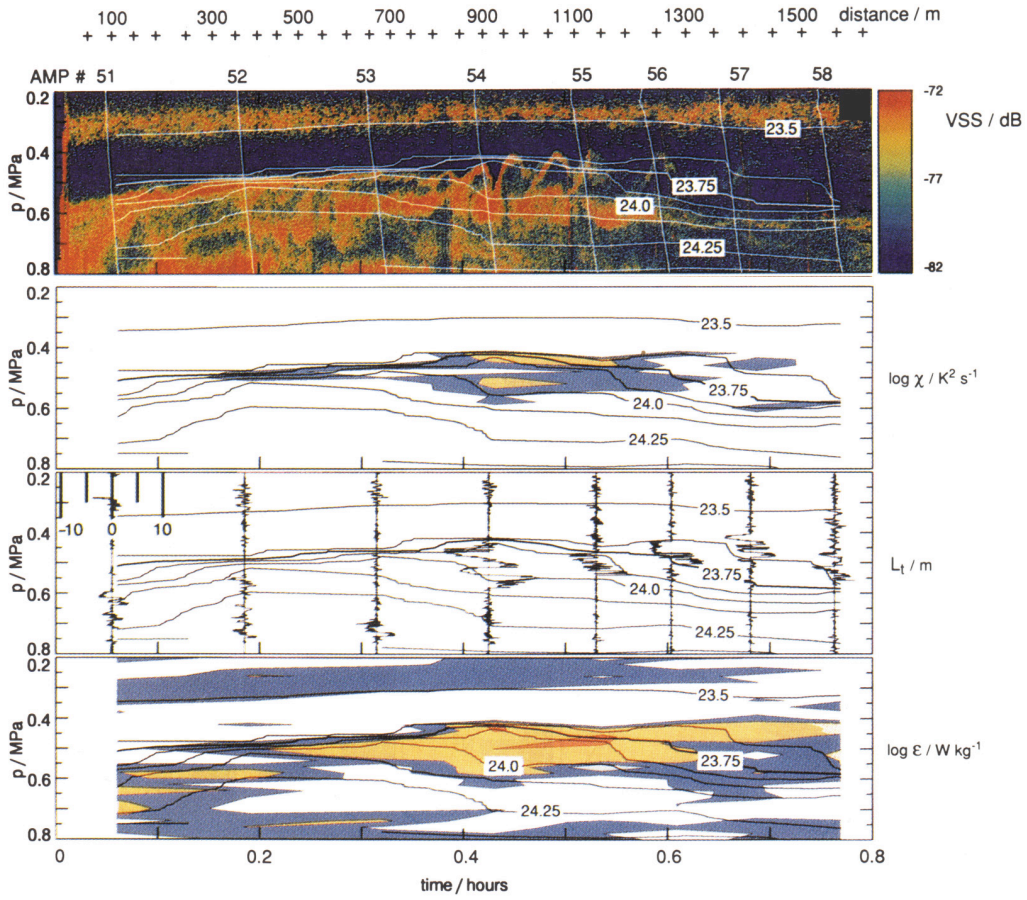

Figure 9: An example of a deterministic turbulent event measured four ways. This is a shear instability, similar in dynamics to the instability in figure 1, observed in Admiralty Inlet, Washington (Seim and Gregg, 1994). a) acoustic backscatter from turbulence microstructure. This visualizes the braids between 0.2 and 0.6 h. Vertical white lines are microstructure profiler drops, horizontal white lines are contours of ρ. b) χ estimated from profiler. c) Density overturns measured with the profiler. Note how there are strong overturns coinciding with the braids. d) The turbulence dissipation rate ε. (For all these panels 0.1 MPa = 10 dbar = 10 m depth)

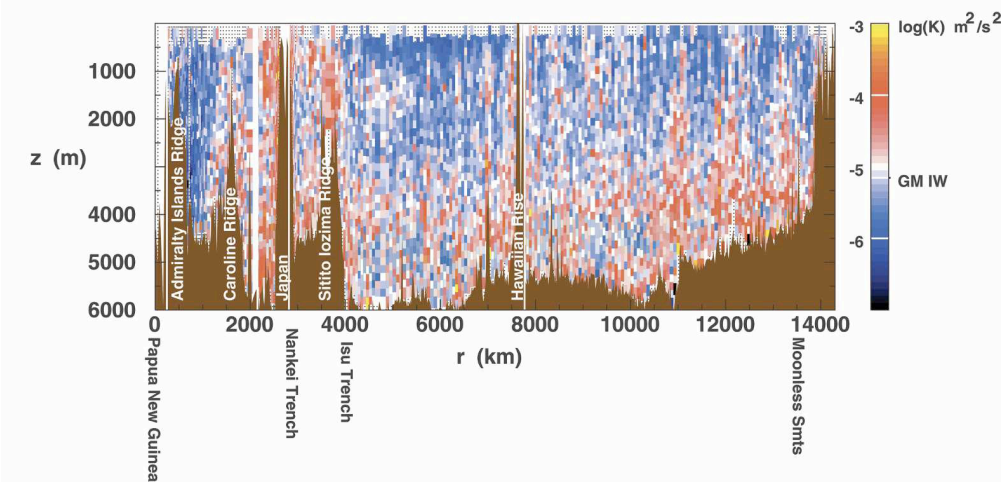

Figure 10: Indirect estimate of mixing from the Western Pacific Ocean using large-scale oceanic data (Kunze et al., 2006). Internal wave energy levels were used to estimate ε, and hence K.